Available online at BCREC Website: http://bcrec.undip.ac.id

Bulletin of Chemical Reaction Engineering & Catalysis, 12 (2), 2017, 281-286

Research Article

Synthesis of SnO_2 Nanoparticles by High Potential Electrolysis

R. Rahmi, Fredy Kurniawan*)

Chemistry Department, Faculty of Mathematics and Natural Sciences, Institut Teknologi Sepuluh Nopember, Jln. Arief Rahman Hakim, Surabaya 60111, Indonesia

Received: 15th November 2016; Revised: 26th February 2017; Accepted: 27th February 2017

Abstract

SnO_2 nanoparticles have been synthesized by high voltage electrolysis. Tin bare was used for anode and cathode. The effect of potentials and electrolyte were studied. The particles obtained after electrolysis was characterized using X-ray Diffraction (XRD). The diffractogram is in agreement with the standard diffraction pattern of SnO_2 which is identified as tetragonal structure. The Fourier Transform Infrared (FTIR) spectrum indicates that there is a vibration of Sn–O asymmetric at 580 cm^{-1}. The optimum potential for SnO_2 nanoparticles synthesis is 60 V at 0.06 M HCl which shows the highest UV-Vis spectrum. The absorption peak of SnO_2 nanoparticles by UV-Vis spectrophotometer appears at about 207 nm. The particle size analysis shows that the SnO_2 nanoparticles obtained have the size distribution in a range of 25-150 nm with the highest volume at 83.11 nm.

Keywords: SnO_2; nanoparticles; electrolysis; high potential

How to Cite: Rahmi, R., Kurniawan, F. (2017). Synthesis of SnO_2 Nanoparticles by High Potential Electrolysis. *Bulletin of Chemical Reaction Engineering & Catalysis*, 12 (2): 281-286 (doi:10.9767/bcrec.12.2.773.281-286)

Permalink/DOI: http://dx.doi.org/10.9767/bcrec.12.2.773.281-286

1. Introduction

SnO_2 is an n-type semiconductor crystal which has a direct band gap of 3.7 eV at 300 K and a high excited on binding energy (130 eV) [1]. SnO_2 has been applied as a catalyst [2], gas sensor [3], battery [4], antibacterial, and antioxidant [5]. These applications are typically used in the form of nanoparticles, e.g. nanosheets [6], nanorod clusters [7], nanorod array [8], nanorod bundles [9], and nanospheres [4] which were prepared by different methods.

Several scientists reported that the SnO_2 nanoparticles could be synthesized using wet chemical methods. Those method are biogenic synthesis [5], gel combustion [10], hydrothermal route [11, 12], sol-gel [13-15], microemulsion [16], solvothermal [17], thermal decomposition [18], sonochemical [19], and precipitation [20, 21]. All methods were proved to produce SnO_2 nanoparticles. Unfortunately, these methods are relatively time-consuming and complicated processes. They are not suitable for fabrication cost and facile preparation process [22]. Another method which can be developed for nanoparticle synthesis is an electrochemical method, which it is proposed in this work. The efficiency of the procedure offers several advantages including control of particles size, excellent yields, operational simplicity and minimum environmental [23]. It has been applied for some research, such as influence CTAB and sonication on nickel hydroxide nanoparticles

Corresponding Author
E-mail: fredy@chem.its.ac.id (Kurniawan, F.)

synthesis [24], synthesis nickel hydroxide by electrolysis at high voltage [25], and influence of $Ni(OH)_2$ nanoparticles on insulin sensor sensitivity [26, 27].

Based on the explanation, most of researchers produced SnO_2 nanoparticles using techniques which require Tin(IV) chloride as a reagent. This reagent is relatively expensive and difficult to be found in Indonesia. There have been limited studies concerned on synthesis of SnO_2 from tin bare which is cheaper and easier to be found in Indonesia. Therefore, this research intent to produce a nano-size SnO_2 using tin bare as the reagent by high potential electrolysis.

2. Materials and Methods

2.1. Materials

Pure tin metal sheets (99.9%) with 1 mm thickness and hydrochloric acid (AR grade 37%) were purchased from Merck. The sheet was adjusted into a dimension of 4 mm × 10 cm before used for anode and cathode. Demineralized water was used for all cleaning and chemical preparation.

2.2. Methods

The SnO_2 nanoparticles were synthesized by electrolysis with a tin sheet as anode and cathode. The scheme of the electrolysis cells is shown in Figure 1. The electrolysis was performed at various potentials, i.e. 10; 20; 30; 40; 50; 60; 70; 80; 90; and 100 V, in 100 mL 0.02 M HCl as electrolyte solution to see the influence of the potential applied. Various concentration of electrolyte solution was also applied to observe the formation of SnO_2 nanoparticles during electrolysis. The concentration was 0.005; 0.01; 0.02; 0.03; 0.04; 0.05; and 0.06 M HCl, at a fixed potential of 60 V. Continues stirring was also applied during all the electrolysis experiment. Electrolysis was stopped after 15 minutes, and then both electrodes were released from the electrolysis cell, dried at room temperature, and weighed to observe the weight different of the both electrodes before and after electrolysis. The solution obtained was also cooled at room temperature and ready for characterization. The plasmon band peak of SnO_2 nanoparticles solution was observed using GENESYS 10S UV-Vis spectrophotometer. The nanoparticles structure was analyzed by Philips X'Pert MPD (Multi-Purpose Diffractometer) XRD using Cu $K\alpha_1$ radiation (λ = 1.540598 nm) and $K\alpha_2$ (λ = 1.544426 nm). The FTIR spectrum was recorded from 4000 to 400 cm^{-1} by a Shimadzu Fourier Transform Infrared (FTIR) spectrophotometer. Malvern Zetasizer Nano Series Instruments was used to measure the particle size obtained.

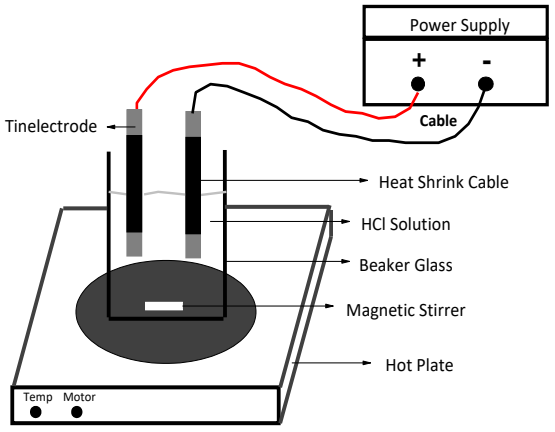

Figure 1. Electrolysis cell for SnO_2 nanoparticles synthesis

3. Results and Discussion

3.1. Synthesis of SnO_2 nanoparticles

The most probable reaction on cathode occurs as Eqn. (1).

Cathode (Sn):

$$2H_2O_{(l)} + 2e^- \rightarrow 2OH^-{}_{(aq)} + H_{2(g)} \quad (1)$$

H_2 production at the cathode can be observed by bubbles formation during electrolysis process. Meanwhile, the reaction on the anode has three possibilities as described in Eqns. (2), (3), or (4):

Anode (Sn):

$$Sn_{(s)} \rightarrow Sn^{2+}{}_{(aq)} + 2e \quad (2)$$

$$Sn_{(s)} \rightarrow Sn^{4+}{}_{(aq)} + 4e^- \quad (3)$$

$$2H_2O_{(l)} \rightarrow 4H^+{}_{(aq)} + O_{2(g)} + 4e^- \quad (4)$$

The oxidation of Sn was observed by the lost weight of the Sn bare (Table 1 shows the mass of tin metal that dissolved during the synthesis process). The Sn can be oxidized to be Sn^{2+} or Sn^{4+}. Formation of O_2 as Eqn. (4) was also observed by the bubbles produced at the surface of the anode.

The nanoparticles were obtained characterized using XRD. The diffractogram is shown in

Figure 2. It has characteristic of 2θ of 26.58°, 33.39°. 36.98°, 52.04°, 62.13°, 64.68°, 73.06° and 78.92°, which corresponding to *hkl* of (110), (101), (200), (211), (310), (112), (202), and (321) for SnO_2 nanoparticles, respectively. The three strong peaks are assigned to the (110), (101), and (211), respectively. All diffraction peaks are in good agreement with the SnO_2 standard diffraction pattern. The results indicate the product obtained is SnO_2 nanoparticles with a tetragonal structure [18].

The FTIR analysis is also in agreement with the SnO_2 spectrum (Figure 3). In this spectrum, the absorption at 934 cm^{-1} is described to surface oxygen of Sn–O [18] and 580 cm^{-1} is assigned to the Sn–O asymmetric vibrations [22]. The presences of two peaks in product confirm the presence of SnO_2. We found that the product has absorption from several functional groups. The peaks at 3396 and 1626 cm^{-1} are assigned to the stretching vibration of OH groups and the bending vibration of absorbed molecular water. Bending vibrations of H–O–H in the water were observed at 1401 cm^{-1}. It also appeared that the absorption at 1159 is assigned to vibration of different types of surface hydroxyl groups. The product in optimum condition (0.06 M HCl at 60 V) was analyzed by zeta sizer (Figure 4). The average size of SnO_2 nanoparticles obtained is 83.11 nm.

3.2. The effect of potential

The optimum conditions in this experiments occurred at the potential of 60 V with the maximum value of absorbance and wavelength are 2.583 and 203 nm, as shown in Figure 5. Comparison with the other potential, in this condition, the greatest mass reduction occurs at the anode. Increasing the applied potential increases the value of absorbance at the maxi-

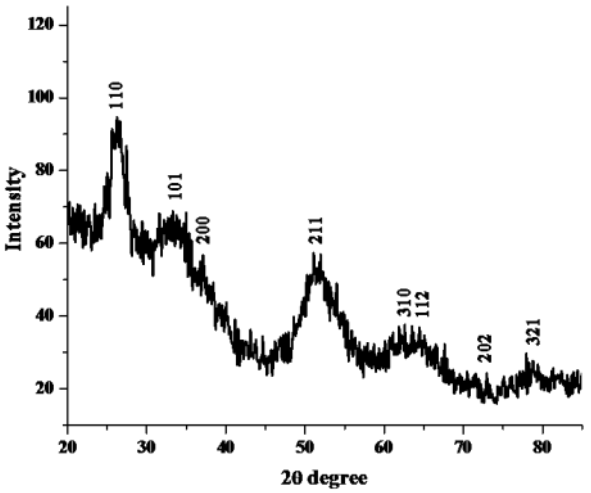

Figure 2. XRD spectrum of SnO_2 nanoparticles

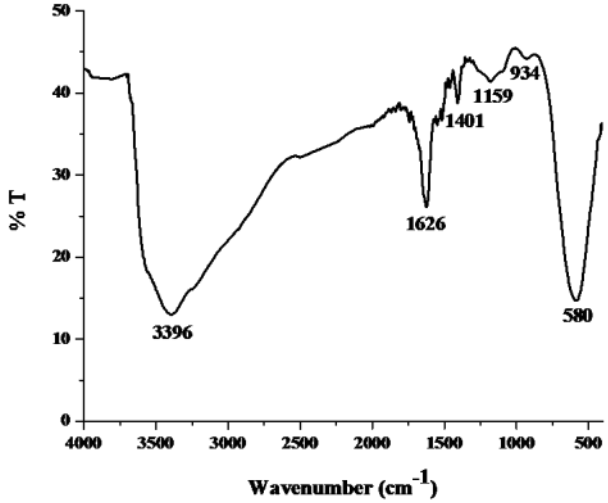

Figure 3. FTIR spectrum of SnO_2 nanoparticles

Table 1. Reduced mass of tin after electrolysis process at various potential in 0.02 M HCl

Potential (V)	Reduce mass of tin (g)
10	0.0171
20	0.0210
30	0.0338
40	0.0399
50	0.0822
60	0.1785
70	0.0835
80	0.1383
90	0.1846
100	0.1668

Table 2. Reduced mass of tin after electrolysis process at various concentration at potential 60 V

Concentration (M)	Tin Mass (g)
0.005	0.0199
0.01	0.0499
0.02	0.1785
0.03	0.1810
0.04	0.2623
0.05	0.2897
0.06	0.2985

mum wavelength. This indicates that the tin bare dissolves more with the potential. This is due to the potential act as a controller parameter in electron pressure that causes a reduction or oxidation reaction [28]. The equation states $E = I.R$, so the greater potential increases the electric current. The electrical current is proportional to the mass of the anode which is oxidized into ions. The ions are only formed under the effect of an electric field that flows through the solution [29].

3.3. The effect of electrolyte solution

Increasing the acid concentration increases the dissolution of tin metal (Table 2). It shows that the greatest mass reduction obtained at 0.06 M HCl. The HCl was ionized into H^+ and Cl^- ions. Whereas, chloride ions from ionization can activate the dissolution of the tin metal (Sn^{2+} or Sn^{4+}) at anode [29]. Observations on the maximum wavelength are presented in Figure 6. UV-Vis spectra show the absorbance value increase with increasing of the acid concentration. It was achieved at 0.06 M HCl with the absorbance and wavelength values are 3.068 and 207 nm, respectively.

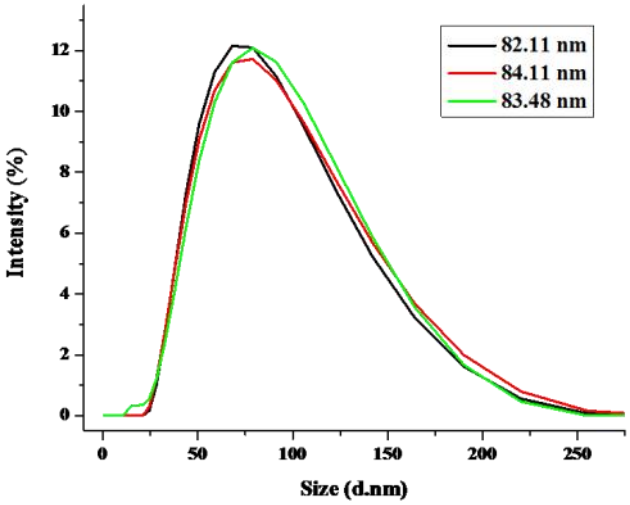

Figure 4. Size distribution analysis of SnO_2 obtained (electrolysis potential 60 V in 0.06 M HCl)

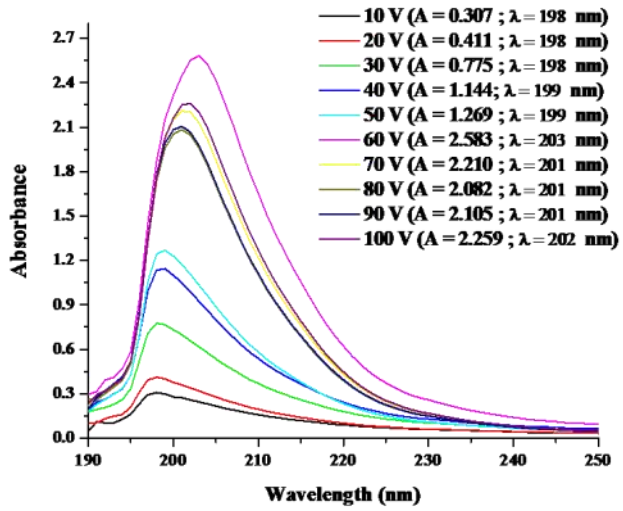

Figure 5. UV-Vis spectrum of SnO_2 nanoparticles at various potentials

The SnO_2 nanoparticles were formed (the oxidation number of tin increase from 0 to 2) in solutions as follows:

$$2H_2O_{(l)} + Sn_{(s)} \rightarrow 2OH^-_{(aq)} + Sn^{2+}_{(aq)} + H_{2(g)} \quad (5)$$

$$Sn^{2+}_{(aq)} + 2OH^-_{(aq)} \rightarrow Sn(OH)_{2\,(aq)} \quad (6)$$

This reaction can be continued to oxidize Sn^{2+} to Sn^{4+} as the following:

$$Sn(OH)_{2\,(aq)} \rightarrow SnO_{2(s)} + H_{2\,(g)} \quad (7)$$

The other possibility reaction can also occur. The oxidation number of tin increases from 0 to +4, the SnO_2 nanoparticles was formed with the following reaction:

$$4H_2O_{(l)} + Sn_{(s)} \rightarrow 4OH^-_{(aq)} + Sn^{4+}_{(aq)} + 2H_{2(g)} \quad (8)$$

$$Sn^{4+}_{(aq)} + 4OH^-_{(aq)} \rightarrow SnO_{2(s)} + 2H_2O_{(l)} \quad (9)$$

4. Conclusions

Based on the results, it was concluded that SnO_2 nanoparticles could be synthesized from the tin metal using an electrochemical method in HCl solution. The optimum condition for the

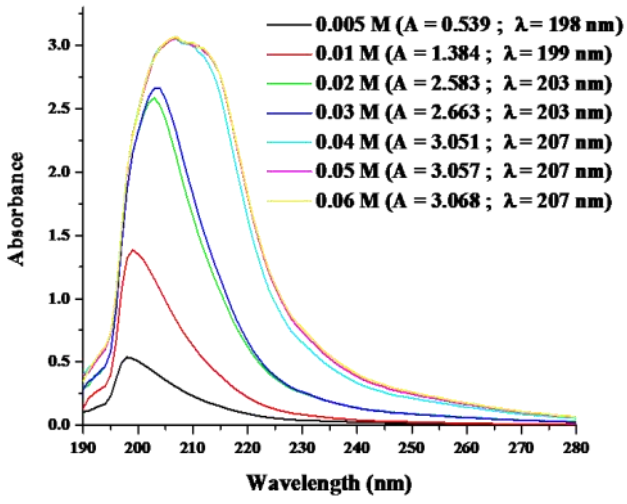

Figure 6. UV-Vis spectrum of SnO_2 nanoparticles at various HCl concentrations

synthesis is at the potential of 60 V. The absorbance value of the conditions is 3.068 at 207 nm. Characterization using XRD indicates the diffractogram pattern of product synthesis is SnO_2 nanoparticles. Furthermore, FTIR analysis also shows the vibration of Sn–O. The particle size of the nanoparticles in 0.06 M HCl is 83.11 nm.

Acknowledgments

The authors are grateful to a DIKTI (Indonesian Directorate General of Higher Education) for support a research fund under the scheme Pra S2-S2 Saintek Scholarship.

References

[1] Gondal, M.A., Drmosh, Q.A., Saleh, T.A. (2010). Preparation and characterization of SnO_2 nanoparticles using high power pulsed laser. *Applied Surface Science*, 256(23): 7067-7070. doi:10.1016/j.apsusc.2010.05.027

[2] Bhattacharjee, A., Ahmaruzzaman, M., Sinha, T. (2015). A novel approach for the synthesis of SnO_2 nanoparticles and its application as a catalyst in the reduction and photodegradation of organic compounds. *Spectrochimica Acta Part A: Molecular and Biomolecular Spectroscopy*, 136: 751-760. doi:10.1016/j.saa.2014.09.092

[3] Mondal, B., Basumatari, B., Das, J., Roychaudhury, C., Saha, H., Mukherjee, N. (2014). ZnO-SnO_2 based composite type gas sensor for selective hydrogen sensing. *Sensors and Actuators B: Chemical*, 194: 389-396. doi:10.1016/j.snb.2013.12.093

[4] Wei, W., Song, L.-X., Guo, L. (2015). SnO_2 hollow nanospheres assembled by single layer nanocrystals as anode material for high performance Li ion batteries. *Chinese Chemical Letters*, 26(1):124-128. doi:10.1016/j.cclet.2014.09.023

[5] Vidhu, V.K., Philip, D. (2015). Biogenic synthesis of SnO_2 nanoparticles: Evaluation of antibacterial and antioxidant activities. *Spectrochimica Acta Part A: Molecular and Biomolecular Spectroscopy*, 134: 372-379. doi:10.1016/j.saa.2014.06.131

[6] Masuda, Y., Kato, K. (2009). Aqueous synthesis of nanosheet assembled tin oxide particles and their N_2 adsorption characteristics. *Journal of Crystal Growth*, 311(3): 593-596. doi:10.1016/j.jcrysgro.2008.09.066

[7] Supothina, S., Rattanakam, R., Vichaphund, S., Thavorniti, P. (2011). Effect of synthesis condition on morphology and yield of hydrothermally grown SnO_2 nanorod clusters. *Journal of the European Ceramic Society*, 31(14): 2453-2458. doi:10.1016/ j.jeurceramsoc.2011.02.018

[8] Zhou, X., Fu, W., Yang, H., Mu, Y., Ma, J., Tian, L., Li, M. (2013). Facile fabrication of transparent SnO_2 nanorod array and their photoelectrochemical properties. *Materials Letters*, 93: 95-98. doi:10.1016/j.matlet.2012.11.050

[9] Wen, Z., Zheng, F., Yu, H., Jiang, Z., Liu, K. (2013). Hydrothermal synthesis of flowerlike SnO_2 nanorod bundles and their application for lithium ion battery. *Materials Characterization*, 76: 1-5. doi:10.1016/j.matchar.2012.11.011

[10] Liu, H., Gong, S., Hu, Y., Zhao, J., Liu, J., Zheng, Z., Zhou, D. (2009). Tin oxide nanoparticles synthesized by gel combustion and their potential for gas detection. *Ceramics International*, 35(3): 961-966. doi:10.1016/j.ceramint. 2008.04.010

[11] Talebian, N., Jafarinezhad, F. (2013). Morphology-controlled synthesis of SnO_2 nanostructures using hydrothermal method and their photocatalytic applications. *Ceramics International*, 39(7): 8311-8317. doi:10.1016/j.ceramint.2013.03.101

[12] Lou, Z., Wang, L., Wang, R., Fei, T., Zhang, T. (2012). Synthesis and ethanol sensing properties of SnO_2 nanosheets via a simple hydrothermal route. *Solid-State Electronics*, 76: 91-94. doi:10.1016/j.sse.2012.05.062

[13] Aziz, M., Saber Abbas, S., Wan Baharom, W. R. (2013). Size-controlled synthesis of SnO_2 nanoparticles by sol-gel method. *Materials Letters*, 91: 31-34. doi:10.1016/j.matlet.2012.09.079

[14] Vijayarangamuthu, K., Rath, S. (2014). Nanoparticle size, oxidation state, and sensing response of tin oxide nanopowders using Raman spectroscopy. *Journal of Alloys and Compounds*, 610: 706-712. doi:10.1016/j.jallcom.2014.04.187

[15] Zhang, J., Gao, L. (2004). Synthesis and characterization of nanocrystalline tin oxide by sol–gel method. *Journal of Solid State Chemistry*, 177(4-5): 1425-1430. doi:10.1016/j.jssc.2003.11.024

[16] Zamand, N., Nakhaei Pour, A., Housaindokht, M.R., Izadyar, M. (2014). Size-controlled synthesis of SnO_2 nanoparticles using reverse microemulsion method. *Solid State Sciences*, 33: 6-11. doi:10.1016/j.solidstatesciences.2014.04.005

[17] Rajendran, V., Anandan, K. (2012). Size, morphology and optical properties of SnO_2 nanoparticles synthesized by facile surfactant-assisted solvothermal processing. *Mate-*

rials Science in Semiconductor Processing, 15(4): 393-400. doi:10.1016/j.mssp. 2012.01.002

[18] Davar, F., Salavati-Niasari, M., Fereshteh, Z. (2010). Synthesis and characterization of SnO_2 nanoparticles by thermal decomposition of new inorganic precursor. *Journal of Alloys and Compounds*, 496(1-2): 638-643. doi:10.1016/j.jallcom.2010.02.152

[19] Yu, Z., Zhu, S., Li, Y., Liu, Q., Feng, C., Zhang, D. (2011). Synthesis of SnO_2 nanoparticles inside mesoporous carbon via a sonochemical method for highly reversible lithium batteries. *Materials Letters*, 65(19-20): 3072-3075. doi:10.1016/j.matlet.2011.06.053

[20] Gaber, A., Abdel-Latief, A.Y., Abdel-Rahim, M.A., Abdel-Salam, M.N. (2013). Thermally induced structural changes and optical properties of tin dioxide nanoparticles synthesized by a conventional precipitation method. *Materials Science in Semiconductor Processing*, *16*(6): 1784-1790. doi:10.1016/j.mssp. 2013.06.026

[21] Ibarguen, C.A., Mosquera, A., Parra, R., Castro, M.S., Rodríguez-Páez, J.E. (2007). Synthesis of SnO_2 nanoparticles through the controlled precipitation route. *Materials Chemistry and Physics*, 101(2-3): 433-440. doi:10.1016/j.matchemphys.2006.08.003

[22] Zhang, J., Wang, S., Wang, Y., Xu, M., Xia, H., Zhang, S., Wu, S. (2009). Facile synthesis of highly ethanol-sensitive SnO_2 nanoparticles. *Sensors and Actuators B: Chemical*, 139: 369-374. doi:10.1016/j.snb.2009.03.024

[23] Anandgaonker, P., Kulkarni, G., Gaikwad, S., Rajbhoj, A. (2015). Synthesis of TiO_2 nanoparticles by electrochemical method and their antibacterial application. *Arabian Journal of Chemistry*. doi:10.1016/j.arabjc. 2014.12.015

[24] Budipramana, Y., Suprapto, Ersam, T., Kurniawan, F. (2016). Influence of CTAB and Sonication on Nickel Hydroxide Nanoparticles Synthesis by Electrolysis at High Voltage. In F. Pasila, Y. Tanoto, R. Lim, M. Santoso, N. D. Pah (Eds.), *Proceedings of Second International Conference on Electrical Systems, Technology and Information 2015 (ICESTI 2015)* (pp. 345-351). Springer Singapore. doi:10.1007/978-981-287-988-2_37

[25] Budipramana, Y., Suprapto, Ersam, T., Kurniawan, F. (2014). Synthesis nickel hidroxide by electrolysis at high voltage. *Research Gate*, 9(11): 2074-2077

[26] Zulkarnain, Z., Kurniawan, F., Ersam, T., Suprapto, S. (2016). Influence of $Ni(OH)_2$ nanoparticles on insulin sensor sensitivity. *ARPN Journal of Engineering and Applied Sciences*, 11(11): 6721-6725.

[27] Zulkarnain, Z., Suprapto, S., Ersam, T., Kurniawan, F. (2016). A Novel Selective and Sensitive Electrochemical Sensor for Insulin Detection. *Indonesian Journal of Electrical Engineering and Computer Science*, 3(3): 496-502. doi:10.11591/ijeecs.v3.i3.pp496-502

[28] Wang, J. (2006). *Analytical Electrochemistry* (Third Edition.) Publication, New York: A John Wiley & Sons, Inc.

[29] Koryta, J., Dvorak, J., Kavan, L. (1993). *Principles of Electrochemistry* (Second Edition.). Publication, New York: A John Wiley & Sons, Inc.

Selected and Revised Papers from The 2nd International Seminar on Chemistry (ISoC 2016) (Surabaya, 26-27 July 2016) (http://chem.its.ac.id/isoc-2016/) after Peer-reviewed by Scientific Committee of ISoC 2016 and Peer-Reviewers of BCREC journal